A Theoretical Study of Substitution Effects in Unimolecular Rectifiers**

By *Robert Stadler,** Victor Geskin,* and *Jérôme Cornil*

The concept of molecular rectifiers introduced by Aviram and Ratner in 1974 has been the starting point of the field of molecular electronics and the possibility of unimolecular rectification has been widely debated ever since. Despite the large amount of publications on this topic over the years, the physical mechanisms leading to this phenomenon have not yet been clarified to the point where a systematic route for enhancing the rectification ratio (RR) of molecules could be suggested. We present here a theoretical study of RR for a range of molecules with a carboxylic group as a bridge between π-conjugated chains substituted by nitro and amino groups to improve the rectification. We estimate the RR in two distinct ways, namely: i) as the ratio of the threshold electric fields required to transfer one electron between the donor and acceptor units of the molecule and vice versa, using quantum-chemical calculations based on the semi-empirical Hartree–Fock Austin Model 1 (AM1) method, ii) as the ratio of the currents in forward versus reverse bias, as obtained with a non-equilibrium Green's function (NEGF) approach for charge transport through gold/molecule/gold junctions within the framework of density functional theory (DFT). The trends in RR as a function of the molecular structure agree very well when these two methods are compared and can be explained in terms of the relative position of the nitro group within the generated electrostatic potential. These findings allow us to derive some general conclusions about the physical mechanisms behind unimolecular rectification.

1. Introduction

Interest in electron transport between nanoscale contacts has recently intensified, in particular due to: i) the advent of the technologically motivated field of molecular electronics;[1–4] ii) recent progress in the experimental techniques for manipulating and contacting individual molecules;[5–8] and iii) the availability of first-principle methods to describe the electrical properties of single molecule junctions.[9–13] Such methods are usually based on density functional theory (DFT) in combination with a non-equilibrium Green's function formalism (NEGF).[14,15]

The field of molecular electronics was initiated in 1974, when Aviram and Ratner introduced a concept for a molecular rectifier based on a single organic molecule[1]. This molecular diode consists of a system with a π-donor and π-acceptor group which are separated by a σ-bonded segment. In this theoretical work, the flow of charges from the cathode to the anode through the molecule was divided into three steps, where the first two are the hopping of electrons and holes from the electrodes to the acceptor and donor parts of the molecule, respectively, and the third is the annihilation of electrons and holes by tunneling through the σ-bridge (see Scheme 1). In this scenario, where the emphasis is put on resonances between energy levels in the system, the annihilation process inside the molecule was not assumed to be responsible for the rectification effect but rather the evolution as a function of the applied bias of the energetic alignment of the Fermi level of the electrodes with respect to the localized highest occupied (HOMO) and lowest unoccupied (LUMO) molecular orbitals on the donor and acceptor parts, respectively.

In an attempt to design large scale circuits with single molecule rectifiers, Ellenbogen and Love tried to reduce the complexity of the rectification mechanism to a single parameter, that is, the energy difference between the LUMO (localized on the acceptor part of the molecule) and the LUMO+1 (on the donor side) at zero bias.[16] The first electron-transport calculations in a coherent regime with a NEGF-DFT technique on such a molecular diode[17] containing nitro and amino groups to define the acceptor and donor parts did not exhibit a large rectification ratio (RR), thus suggesting that this design scheme was too simplistic. Recently, another NEGF-DFT study on similar molecules yielded a larger RR (around 3–4 when averaging the ratios of forward and reversed bias currents at four voltages between 0.5 and 2 V); the authors argue that the rectification can only be found if the σ-bridge is replaced by a π-bridge.[18] We will refer to this work later and contrast it with our own results.

[*] Dr. R. Stadler, Dr. V. Geskin, Dr. J. Cornil
Laboratory for Chemistry of Novel Materials, University of Mons-Hainaut
Place du Parc 20, B-7000 Mons (Belgium)
E-mail: r.stadler@averell.umh.ac.be

WILEY
InterScience®
DISCOVER SOMETHING GREAT

Several experiments found a rectification in the current–voltage curves of metal/molecule/metal junctions.[19–22] This effect, however, can have different origins in the nanojunction:[23,24] i) an asymmetry in the coupling of the molecule to the two electrodes.[25,26] This effect can be explained by charging effects that depend on the energetic positions of HOMO and LUMO relative to the Fermi levels of the electrodes. The dependence on bias direction arises from the fact that the charge transfer at equilibrium, which defines the level alignment at zero bias, mainly occurs between the molecule and the electrode to which it is the most strongly coupled;[26] ii) an asymmetry of the molecular structure caused by a difference in the length of attached alkyl chains, which places the conjugated unit crucial for charge transport closer to one electrode than the other;[27,28] it has been shown that a single active molecular level is sufficient for this type of rectification;[27] and iii) a rectification effect which is defined by an asymmetry of the electronic density of the relevant molecular orbitals (MOs) in the conjugated core, that is, a unimolecular rectification. Only (iii) is in the spirit of the original Aviram–Ratner proposal and relates to the tailoring of electronic states. The three theoretical articles discussed in the last paragraph[16–18] deal with molecules belonging to this category.

It has to be mentioned that, although unimolecular rectification is nowadays usually envisioned to take place in the strong coupling regime of coherent tunneling (whereas the original work of Aviram and Ratner[1] allows for a broader definition), there are also proposals for diodes based on a Coulomb blockade behavior,[29] a Debye screening in electrochemical systems,[30] a multi-phonon suppression[31] and intermolecular non-adiabatic electron transfer processes.[32] These ideas do not fall into the scope of our article, which focuses exclusively on the physical mechanisms of unimolecular rectification for a single molecule strongly coupled to two metal electrodes in a vacuum environment.

We present here a systematic investigation of unimolecular rectification and analyze structure–property relationships for a selection of asymmetric molecules (Fig. 1). All molecules in Figure 1 have a carboxylic group as a bridge between the π-conjugated acceptor and donor segments; this group introduces asymmetry even in the absence of functional side-groups. In our study, we focus particularly on the rectification enhancing effect of NO_2- and NH_2-groups attached to the acceptor and donor sides, respectively, and on the influence of their position relative to the carboxylic bridge in the middle of the molecule. Our results have been obtained by employing two different computational techniques. In order to separate intramolecular factors from effects related to contacts in a junction, we started our study by using the semi-empirical Hartree–Fock (AM1) method[33,34] coupled to a configuration interaction scheme, as implemented in AMPAC[33] to analyze the field-dependent charge transfer processes inside the isolated molecules. We then corroborate our findings by employing a NEGF-DFT approach[9,35,36] for electron transport through gold/molecule-dithiolate/gold nanojunctions under finite bias.

2. Results

2.1. Computational Approaches

The two methods that we used in this work vary significantly in three aspects. First, AM1 is a quantum-chemical technique that allows for the description of electronic excitations in the framework of a configuration interaction (CI) scheme. In contrast, with NEGF-DFT, the ground-state electron density under a given external potential (when including an applied field) is the central variable. Second, AM1 is a parameterized approach, which makes it computationally very efficient for systems for which reliable atomic parameters are available, that is, all organic molecules but only a rather small selection of metals. By contrast, DFT calculations do not require parameters fitted to experiments,[36] which has the advantage that the issue of transferability of such parameters to different systems or different physical boundary conditions never arises;
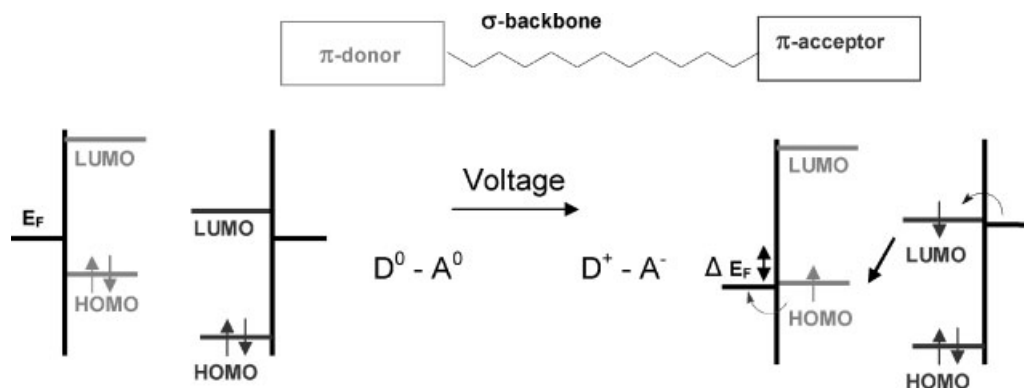
Scheme 1. Illustration of the original Aviram-Ratner concept in Ref. [1]. The key feature is the energetic alignment of the Fermi level E_F of the electrodes with the local HOMO and LUMO levels on the π-donor and acceptor units, respectively. In this simple model, the energy difference between these local levels at zero bias determines which voltage direction gives rise to the largest current.
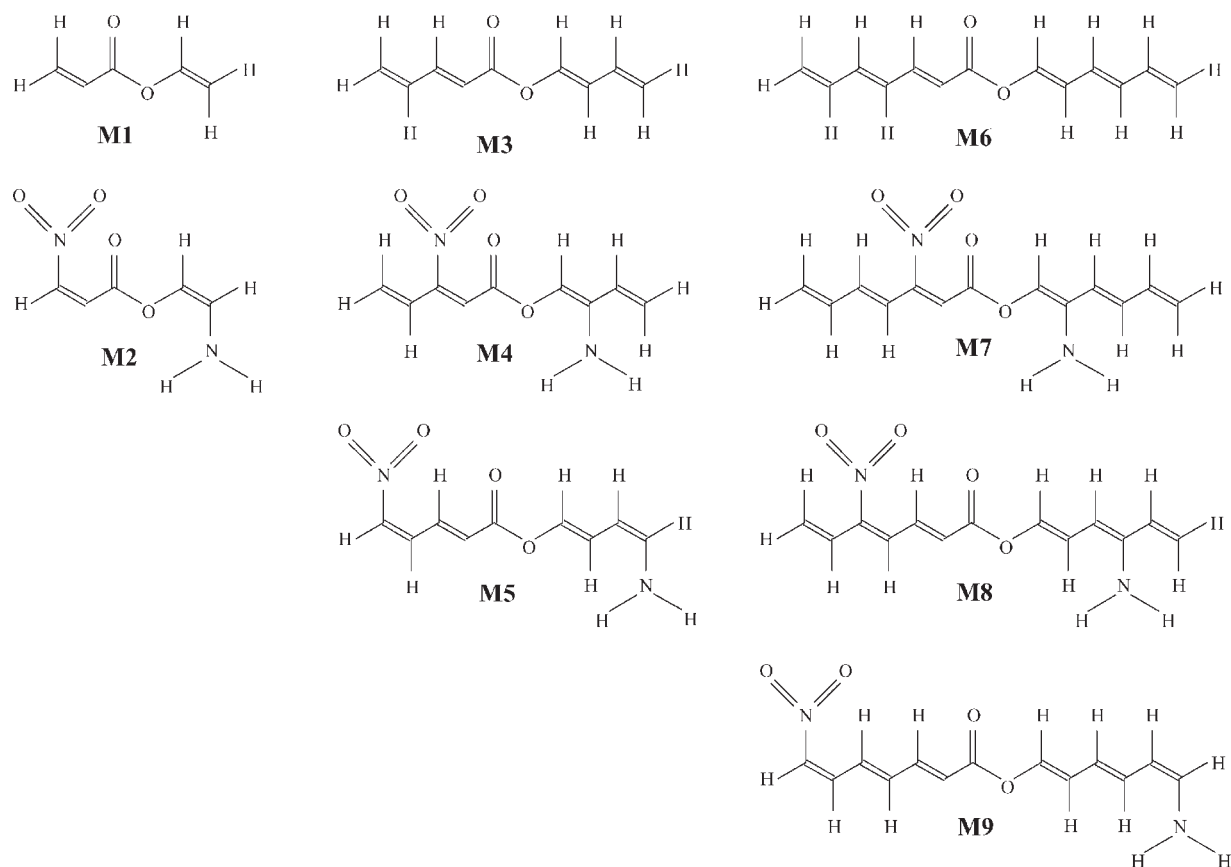
Figure 1. Chemical structures of the unimolecular rectifiers under consideration in this article.

however, this comes at the cost of being computationally very demanding. The third difference is the most crucial one for this work: with AM1, we shift charges between the donor and acceptor sides inside the isolated molecules, whereas with NEGF-DFT, we solve the non-equilibrium problem of a current passing from one electrode to another through the molecule.

2.1.1. Rectification Ratios from Threshold Electric Fields in AM1

One way to define an RR from AM1 calculations (which describe the charge distribution of an isolated molecule under the influence of an external perturbation) is via Mulliken charges N_{mull} on the acceptor and donor segments of the molecule. We exemplify our strategy in Figure 2 with molecule M1 (Fig. 2a) as an example. We use so-called sparkles as the external perturbation,[33] that is, we place two point charges of opposite sign 6 Å away from the two terminating atoms of the molecules. Because these point charges are sufficiently far away from the molecule, this perturbation mimics the effect of a homogeneous electric field. The charge of these sparkles defines the x-axis in Figure 2b–d. The figure demonstrates that the field-dependence of N_{mull} values calculated over the entire

donor and acceptor sides of the molecule mirror each other and exhibit a step structure for CI calculations: at a given threshold field, an electron jumps from one side of the molecule to the other. This threshold value can be unambiguously defined from the inflexion points of N_{mull} versus the sparkle charge or in other words from the maxima in d N_{mull}/dQ (Fig. 2c). N_{mull} does not vary with the external field over the carboxylic group, which plays the role of the bridge for the electron transfer. RR is here defined as the ratio of the threshold values in the forward and reversed bias directions, which are obtained by an inversion of the signs of the sparkles at the opposite ends of the molecule. We will show that these RR values for intramolecular charge transfer are directly related to those computed for coherent transport through the same molecule coupled to two electrodes.

The field strength needed for electron jumps in Figure 2b must be related to the crossing of many-electron ionization and affinity levels taking place when the eigenenergies of Hartree Fock (HF) levels belonging to the two parts come close enough. We stress that a closed-shell HF ansatz cannot describe such electron transfer processes properly and that a CI description including excitations among a few frontier occupied and unoccupied MOs is required to access these many-electron states for the correct description of electron jumps.
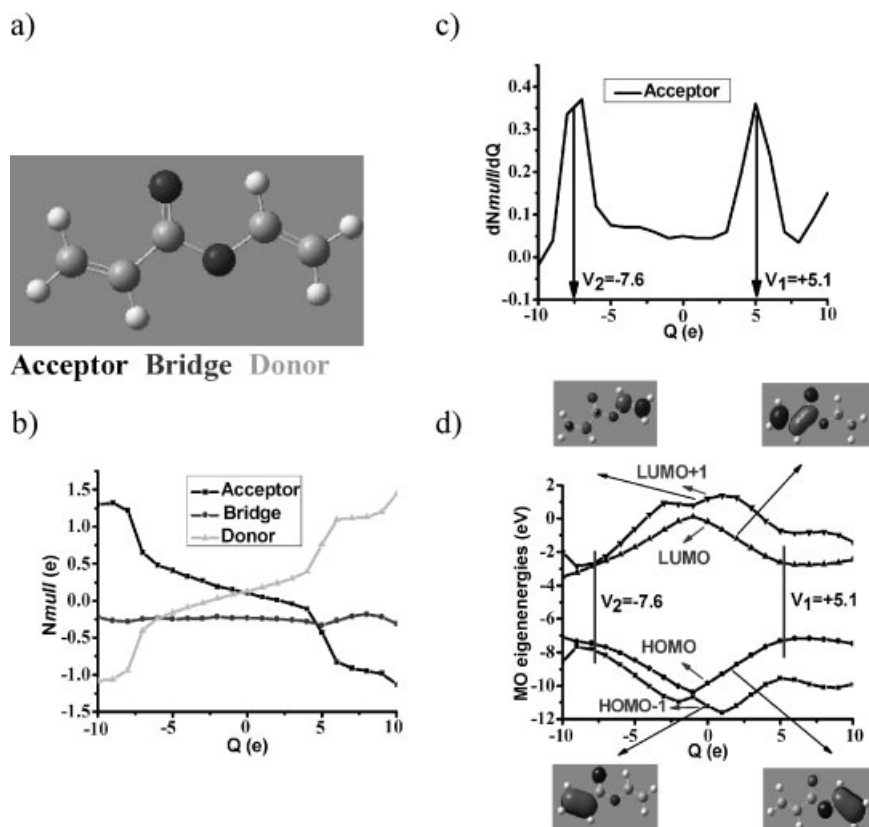
a)

Acceptor Bridge Donor

b)

c)

d)

Figure 2. Illustration of the way RRs can be obtained with AM1: a) definition of the acceptor, bridge, and donor segments in molecule M1 (see Fig. 1); b) Mulliken charges on each molecular segment of M1 as a function of the sparkle charge (see text); c) definition of threshold values from d N_{mull}/dQ; d) shift of MO levels as a function of Q. The sign of Q in b), c) and d) is defined in such a way that the electron moves towards the positive pole.

Fig. 2d); one can distinguish MOs on the donor and acceptor sides, respectively, from the sign of the slope. We will show later that this similarity in slopes is not a general case and that differences in spatial distributions of MOs play a crucial role in our study. For sake of simplicity, we will refer to avoided crossings at the threshold values as *level crossings* throughout this article.

In all AM1 calculations, the molecular geometries have been optimized at zero bias but the atomic positions have not been relaxed in the presence of the sparkles in order to focus only on purely electronic effects at this stage.

2.1.2. Rectification Ratios from I–V Curves Using a NEGF-DFT Method

From NEGF-DFT calculations, we derive a current through a gold/molecule-dithiolate/gold junction (see Fig. 3a for molecule M1) as a function of an applied bias; the results can be directly compared to the current–voltage (I–V)-characteristics measured in experiments.[9,35] Figure 3b shows such a calculated I–V curve for M1. With this approach, we can define RR as the ratio of the currents in the forward and reversed bias directions at each voltage. In Figure 3c, it can be seen that, although there is some fluctuation in RR with the bias, it is an order of magnitude smaller than RR itself. In the following, we have calculated the average of RR for four different voltages (see caption of Fig. 4) in order to be able to compare the trends with the AM1 results, where we get just one RR value according to the threshold voltage definition.

In order to compute the current with the NEGF-DFT formalism, the transmission function T has to be integrated over the bias window for a junction with its electron density polarized by the generated electric field.[9,35] For the single molecular junctions considered in this article, T was calculated using a general non-equilibrium Green's function formalism for phase-coherent electron transport,[15] where both the Green's function of the scattering region and the self-energies describing the coupling to the semi-infinite electrodes were evaluated in terms of localized basis functions.[36] Explicit examples of such transmission functions are shown in the discussion section. In our calculations, the supercells for the scattering region are defined by 3×3 atoms in the direction perpendicular to the transport direction and contain three surface layers on each side of the molecule. We found that a 3×3 k-point grid is needed for the sampling in the transverse

For this reason, it is hard to identify the threshold electric fields in the evolution of the HF MO eigenenergies with the applied field where they appear as avoided crossings (marked by vertical lines), as exemplified in Figure 2d. However, such MO eigenenergy diagrams can serve as a tool for the analysis of intramolecular energy jumps that we will exploit in the discussion section. When the composition and location of an MO remains sufficiently unchanged with the applied field, its eigenenergy varies linearly with the external electric field. Deviations from linearity thus indicate the fields at which changes in MO composition take place (as corroborated by the analysis of the spatial distribution of these MOs) and allow for the identification of a few frontier MOs essential for the description of the electron jump. In the simple case of molecule M1, only the highest two occupied (HOMO, HOMO−1) and the lowest two unoccupied orbitals (LUMO, LUMO+1) of the molecule participate in the charge transfer; their eigenenergies evolve nonlinearly with the field in the vicinity of the threshold charge values, as shown in Figure 2d. The situation is even further simplified for M1, where a similar slope is found for all four relevant MOs in the linear region of their field evolution. This is rationalized by the fact that these four MOs are all π-states with similar spatial distributions (see the insets of
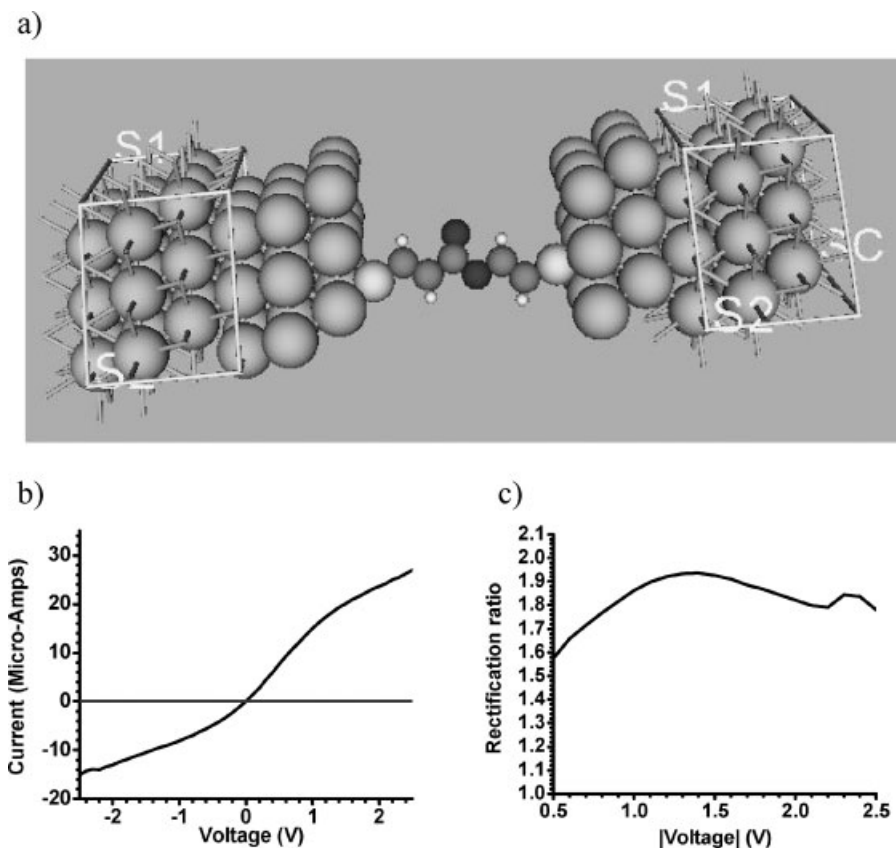
Figure 3. Illustration of the way RRs can be obtained with a NEGF-DFT technique: a) single-molecule nanojunction with M1 (see Fig. 1) connected to gold electrodes via thiolate groups; b) calculated I–V curve for this junction; c) RR obtained as the ratio of the current in forward and reversed bias directions as a function of the applied voltage. For b) and c), the calculations have been performed for voltage steps of 0.1 V.

ruling out effects of differences in the implementation of basis sets. With Gaussian we also compared sparkle charges with homogeneous electric fields on a CI level and found absolute numerical correspondence.

Figure 4a compares the threshold voltages obtained with the semi-empirical AM1 technique (black squares) and with the ab initio CI calculations (bright circles). Although the voltages are in general larger at the ab initio level, their ratios and therefore RR are almost identical when compared to AM1 (around 1.5).

The justification of using DFT is less straightforward since it is not relevant to perform CI calculations on systems containing metallic electrodes as the treatment of electron transport in NEGF-DFT requires. However, we can compare N_{mull} in the range of field strengths associated to the voltages in all I/V curves, see Fig. 4b. Note that the x-axis in Fig. 4b covers a range of field strengths corresponding to sparkle charges of about ±5 |e|; the values representative of the bias in NEGF- DFT calculations on metal/molecule/metal junctions is only ~0.1–0.2 V Å^{-1}. In this limited range, the slope of the DFT curve is higher than that obtained at the ab initio CI level; N_{mull} is overestimated by an almost constant factor of ~1.4 with DFT so that the difference between the two approaches cancels when calculating RR.

It would seem natural to perform all calculations in this work, including the study of threshold voltages for intramolecular electron jumps, on the basis of a DFT framework. It is, however, well known that, due to the lack of a derivative discontinuity in the exchange correlation functional, DFT describes such jumps in a physically incorrect way.[40] It is only in the low bias regime for rather strongly coupled junctions, where no such jumps occur, that DFT-based methods can be trusted to give reliable results. Therefore, we have limited the comparison of DFT with ab initio CI to the linear region in Fig. 4b.

2.2. Trends in Rectification Ratios

2.2.1. Comparison of the Rectification Ratios

In Fig. 5, the rectification ratios derived from AM1 (squares) and NEGF-DFT (triangles) are compared for the nine molecules. We did not perform NEGF-DFT calculations for molecules M2, M5, and M9, since the nitro groups would have

Brillouin plane in order to obtain sufficiently accurate results for T and the current. The atomic configurations used for the molecular structures in all junctions are those relaxed at zero bias at the AM1 level and attached to the gold electrodes with thiolate groups; the sulfur atoms have been placed in a hollow position with respect to the surface plane at a vertical distance of 1.7 Å.[37,38]

2.1.3. Justification of Using AM1 and NEGF-DFT on Different Voltage Scales

Since the two methods employed in this work for studying RR are based on different theoretical frameworks (and different approximations) for the electronic structure description, it is useful to evaluate their reliability for the tasks associated to our study. This was done by benchmarking the performance of both methods with respect to highly accurate ab initio CI calculations (complete active space – self consistent field involving excitations among several frontier orbitals and using the 6-31G** basis set) with the Gaussian software;[39] the latter has also been employed for the DFT results (within the local density approximation) presented in this subsection for
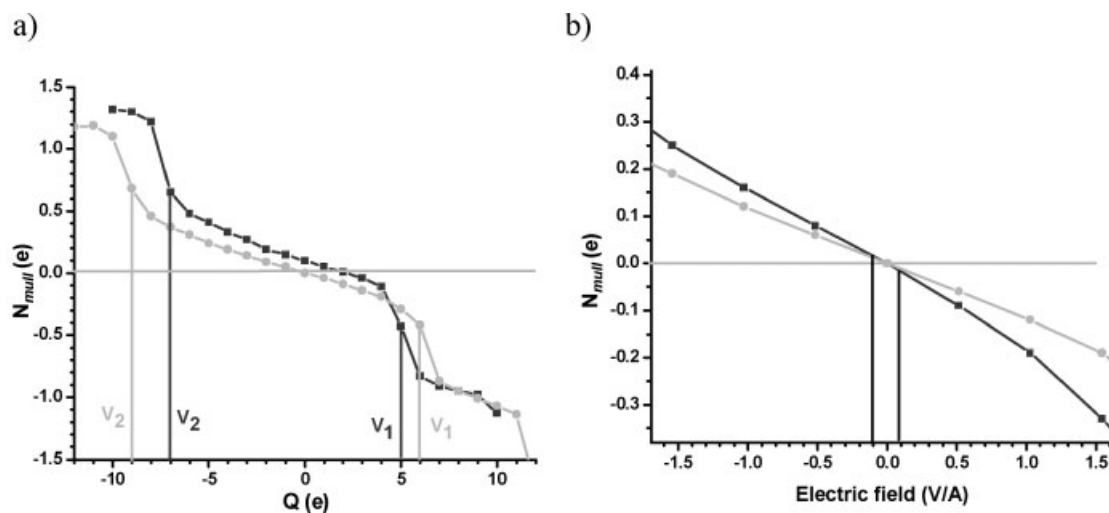
Figure 4. Comparison of a) N_{mull} versus sparkle charge from AM1 and b) N_{mull} versus electric field from DFT with results obtained from ab initio CI calculations (bright circles in the two plots) for molecule M1 in Fig. 1. Note that the range covered by the x-axis in b) is smaller by about a factor of two than in a). The threshold voltages are highlighted in a) while the range of field strength corresponding to a bias of +/−1V in the metal/molecule/metal junctions is marked by vertical lines in b).

been in direct contact with the gold surface. Strikingly, the general trends obtained for RR as a function of the molecular structure are similar with both computational approaches. This has two important implications: first, in contrast to the assumption made in the original Aviram-Ratner proposal,[1] the energetic alignment of the molecular levels with the Fermi energy of the electrodes cannot be the sole decisive factor when the rectification properties of different molecules are compared. Although this probably plays a significant role for a quantitative assessment, our results suggest that the variations in RR for different molecules must have an intramolecular origin otherwise AM1/CI calculations would not reproduce the

Figure 5. RRs calculated with AM1 (squares) and NEGF-DFT (triangles). For the NEGF-DFT results which are voltage dependent (see Fig. 3c), the average of the current ratio at 0.5, 1, 1.5, and 2 V has been used. The electrostatic potential at the position of the nitrogen atom of the nitro group in the AM1 calculations for sparkles with charges $Q = \pm 1$ is shown as circles. The x-axis refers to the labeling of the molecules in Fig. 1.

trends found with NEGF-DFT. Of course, we only draw here conclusions for the molecules studied in this article and do not claim that our results can be readily applied to every possible single molecule junction. It has to be noted that the calculated RR are rather small compared to some experimental measurements,[19–23] for which it is not so easy to determine whether the observed effect comes from unimolecular rectification only. However, there are some characteristic features in the selected molecular structures that are found in the unimolecular rectifiers described so far in the literature.[16–18] Namely, we use gold electrodes, thiolates as anchoring groups, and a molecule with a π-conjugated molecular backbone and nitro and amino groups to induce acceptor and donor segments. The second conclusion is that AM1 appears to be a good screening tool for investigating rectification behavior in single molecular junctions. Once again, it is worth stressing that this picture might differ for another set of molecules. However, this approach is very attractive since AM1 calculations run for only a few seconds whereas the NEGF-DFT calculations required to produce the results in Figure 5 take several days.
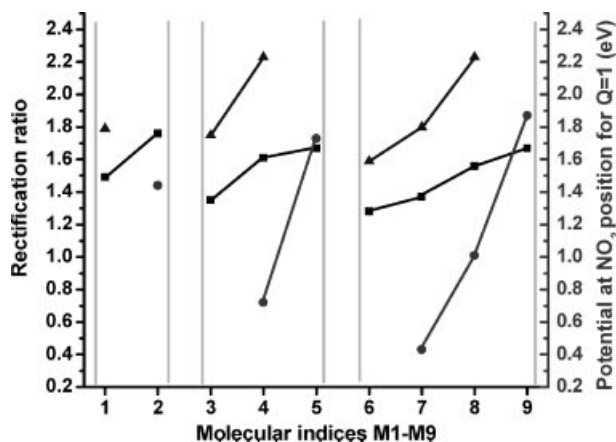
2.2.2. Geometry Dependence of the Electrostatic Potential

To further analyze the structure-property relationships obtained in Figure 5, we recall that RR relies on a strong asymmetry of the electronic density of some relevant MOs. The nature of the MOs that play a crucial role in the rectification process for the molecules under investigation will be the main topic of the discussion section. As expected, the results demonstrate that the nitro and/or amino groups are important in defining the actual localization pattern of the relevant MOs, since our structural variations for a given chain size consist only

in changing their distance from the central carboxylic bridge. We will show hereafter that only the nitro group has actually a significant electron density in the MOs close to the HOMO–LUMO gap. From Coulomb's law, we can derive the electrostatic potential induced by the sparkle charges at a given point along the molecular backbone in the AM1 calculations. In Figure 5, we have plotted this electrostatic potential at the position of the nitrogen atom in the NO_2 group as circles on a different scale compared to the RR data. The resulting curve follows the general trend observed with RR, that is., with the substituents moving closer to the electrodes, the electrostatic potential at the NO_2-position increases and RR is enhanced. There is, however, another feature in the AM1 results (squares in Fig. 5) which is not captured by pure electrostatics. For molecules M5 and M9, (those where the substituents are positioned at the largest distance from the bridge, see Fig. 1), the rise in RR seems to reach a limit and is indeed smaller than the slope going from M3 to M4 or from M7 to M8, respectively. This feature cannot be explained just on the basis of electrostatic arguments and its quantum-chemical origin will be demonstrated in the next section.

We point out that the two molecules studied in Refs. [17] and [18] also differ in their structure by the localization of the functional groups with respect to the electrodes. This observation might provide an explanation for the differences in RR between these two junctions which does not rely on the presence of a saturated *versus* conjugated bridge, as claimed by the authors of Ref. [18]. Despite the fact that the current through a single molecule junction is indeed reduced when a π-bridge is replaced by a σ-bridge, there is no apparent reason why the reduction in the conductance should be more pronounced for the forward bias than for the reversed bias direction.

The importance of the spatial position of a chromophoric group inside single molecule junctions under bias has been recognized before in the context of scanning tunneling microscopy[41] (where the coupling of the central molecule to the two electrodes is asymmetric) and monolayers of molecules with terminal alkyl chains of different lengths, both considering a single[27] or two MOs[42] in the central moiety in simple tightbinding models. To the best of our knowledge, the effect of molecular geometry and of the relative position of chemical groups in an electric field on the rectification properties has not been discussed in detail so far at a quantum-chemical level or within a NEGF-DFT electron transport formalism.

3. Discussion

3.1. Field-Induced Shifts of MO Levels

In Figure 2, we have established for the AM1 calculations a connection between the local Mulliken charges on the donor and acceptor sides of an asymmetric molecule and the crossings of MOs when an electric field is applied. Such a connection has also been made between the peaks in *I–V* curves calculated

with the NEGF-DFT method and the bias-induced crossings of Kohn-Sham orbitals.[17] In a recent DFT-based study of the rectification properties of an asymmetric molecule, the slopes of the evolution of different electronic level energies with the bias have been rationalized in terms of the polarizability of the different halves of the molecule[43] (including the gold clusters they were attached to and the resulting screening effects).

Before undertaking a direct comparison of MO level shifts calculated from AM1 and NEGF-DFT, differences between the two methods have again to be stressed. On the one hand, it is well-known that DFT methods underestimate the HOMO–LUMO gap in general, whereas our AM1-calculations are likely to overestimate them. On the other hand, the actual level energies with NEGF-DFT are also influenced by the orbital-dependent coupling to the electrodes. Our comparison can therefore be only qualitative in nature. Note also that we perform the two analyses in a different range of applied voltages, since -as we will show below- the levels do not actually have to cross within the NEGF-DFT formalism to explain the trends in RR found in Fig. 5.

3.1.1. AM1

In Figure 6, we display the field-dependent MO level shifts from our AM1 calculations for molecules M6–M9. The spatial distributions of the MOs participating in the charge transfer for voltages applied in both directions are also shown as insets. The only orbital changing its localization pattern when moving the position of both side-groups is the LUMO in the forward bias direction (see the right side in Fig. 5a–d), which is centered around the NO_2-group. In turn, this change of localization steepens the slope of the corresponding energy evolution with the bias when the NO_2-group moves from the center towards the end of the molecule. Since the potential at a given point induced by two oppositely charged sparkles is given by $V = Q(1/R_1 - 1/R_2)$, where $\pm Q$ are the sparkle charges and $R_{1,2}$ are the corresponding distances, it is clear that in the middle $(R_1 = R_2)$ $V = 0$ for any charge Q; however, there is an increase in the slope of V versus Q (and hence in the eigenenergy of an MO localized around that point) when moving away from the center. A higher slope therefore leads to an earlier crossing with the unchanged HOMO level. No such effect induced by the nitro group is found in the orbitals for the reversed bias, thus explaining why there is an increase in the rectification going from M6 to M9. Figure 6d also reveals why the rectification enhancing effect is diminished with the AM1 results in Figure 5 for molecule M9. In this case, the slope has become so steep for all orbitals with a strong localization on the nitro group that the HOMO–6 (with a large amplitude on NO_2) crosses easily the LUMO under reversed bias, thereby partially balancing the ratio enhancement driven by the forward bias.

We want to contrast our findings with the model proposed by Ellenbogen and Love: [16] whereas the energy difference between the LUMO (on the acceptor side) and the LUMO+1 (on the donor side) at zero bias is suggested in Ref. [16] to be the
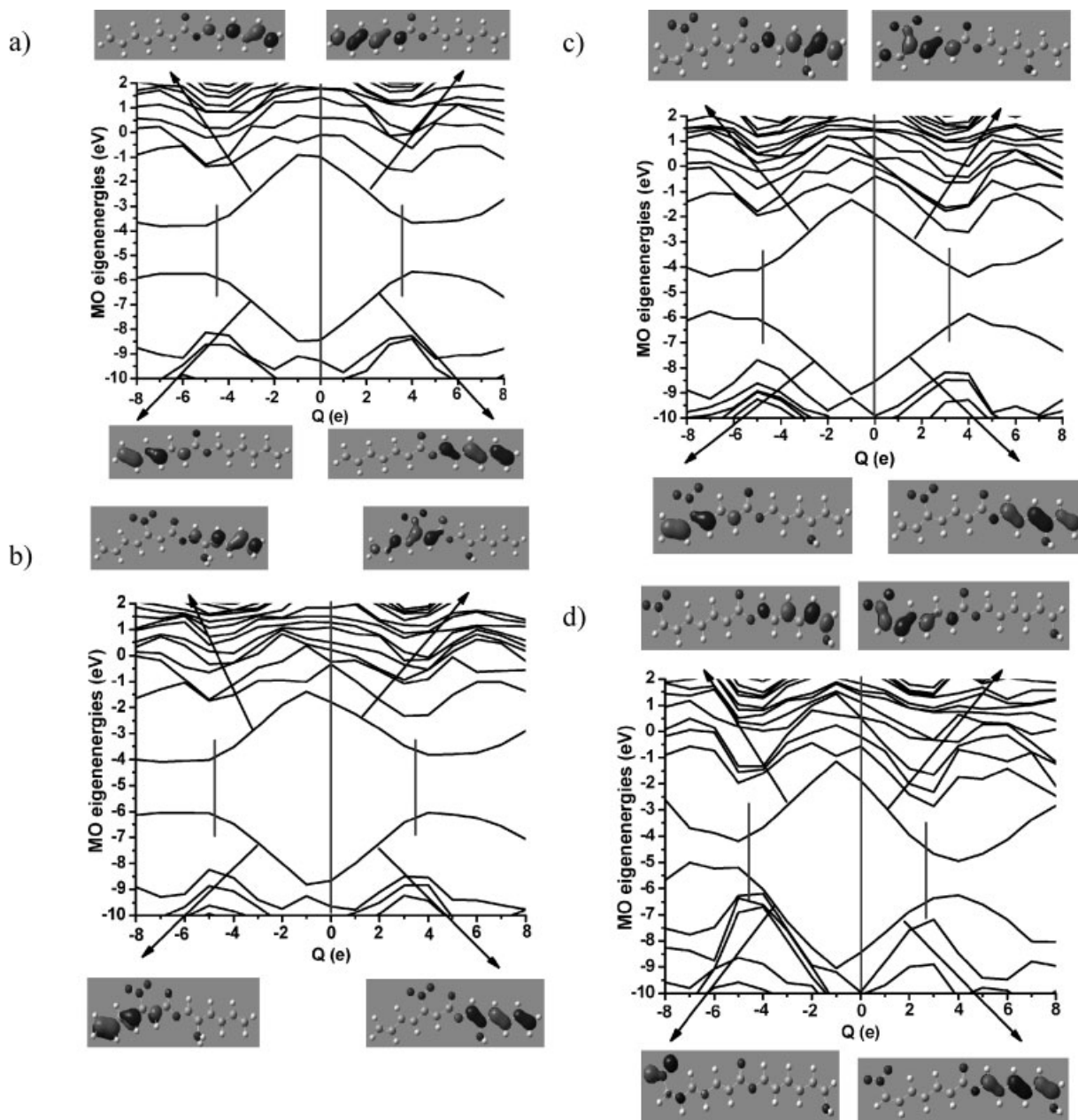
Figure 6. Evolution of the MO eigenenergies as a function of the sparkle charges (see Fig. 2d), as computed with AM1 for molecules a) M6, b) M7, c) M8 and d) M9 (see Fig. 1). The vertical lines indicate the charge sparkle promoting the electron transfer, as obtained from the Mulliken charges calculated at the AM1/CI level.

energetic quantity to optimize, we claim from our results that it is crucial to look at the field-dependent evolution of all MO eigenenergies. It does not have to be necessarily the LUMO which plays the central role in the crossing of levels and in changing the rectification ratio.

3.1.2. NEGF-DFT

In Figure 7, we show the eigenvalues of the self-consistent Hamiltonian projected on the molecular part in the NEGF-

DFT calculations for molecules M6-M8; this has been computed by diagonalizing the sub-Hamiltonian of the central region defined with the basis functions localized on the molecules.[9,17] In marked contrast to Fig. 6, where we plotted the MO level shifts in a range of electric fields going beyond the level crossings, we limit the extent in Figure 7 to much smaller voltages corresponding to those that could be realistically achieved in experimental I–V measurements.

For comparing the relevant features for the three molecules in Figure 7, the three orbitals which require attention are highlighted by showing their spatial distributions in the insets.
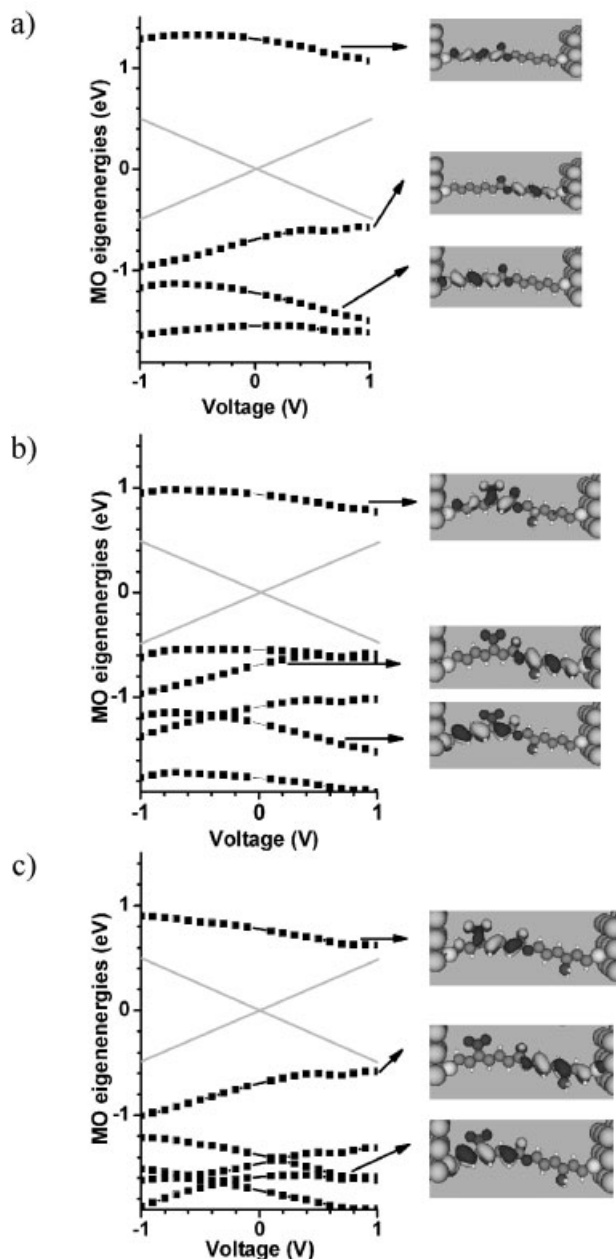
Figure 7. Evolution of the MO-eigenenergies as a function of the external bias, as calculated with the NEGF-DFT formalism for molecules a) M6, b) M7 and c) M8 (see Fig. 1). The diagonal bright lines indicate the bias window.

These are the LUMO, HOMO and HOMO-1 for molecule M6; for the other molecules, additional MOs localized on the oxygen atoms of either the nitro or carboxylic moieties also come close to the Fermi level but have not been found to contribute to the transmission functions in Figure 8 (see below). In deep parallelism with Figure 6, it is also here only the LUMO level which exhibits significant changes in its localization pattern and energetic evolution when the molecules in Figure 7 are compared. We also note that the shapes of

all the relevant orbitals perfectly match the corresponding ones calculated at the AM1 level. For molecule M6, the LUMO remains far above the bias window (indicated by diagonal lines) when integrating the transmission function for both bias directions whereas the LUMO is energetically lowered in molecules 7 and 8, thereby approaching the integration window and in the case of M8 falling below for a forward bias of slightly more than +1V (the actual crossing point is not displayed in the figure).

3.2. Transmission Functions and the Role of Coupling to the Electrodes

The most important physical quantity calculated in NEGF-DFT calculations for electron transport through single molecular junctions is the transmission function T.[9–13] Its value at the Fermi energy defines the zero-bias conductance and its integral over the bias-dependent energy window gives the current. In Figure 8, we have plotted T at three different voltages for molecules M6, M7, and M8. The voltage-dependence in a calculated *I–V*-curve (see Fig. 3b for example) is twofold. On the one hand, there is the trivial effect of the size of the bias window (shown as vertical lines in Fig. 8), which cannot by itself generate rectification since it does not depend on the direction of the applied bias. On the other hand, T also changes when a voltage is applied since the electronic structure of the junction is polarized by the field; this polarization has to be asymmetric to induce a rectification in the *I–V* curves. The energetic shift of MOs upon application of a voltage, as discussed in the context of Figure 7, has an impact on T (by shifting the energetic positions of the peaks), but does not determine T entirely since no information about the coupling between MOs and the orbitals of the electrodes (that defines the width of the peaks) can be obtained from the sole consideration of the MO level positions.

The overall impression given by Figure 8 is that the shape of the transmission spectrum changes considerably with the applied field for the three molecules but in a very similar way for each structure. The only exception is around the energetic position of the LUMO peak at about +1 eV. This peak is totally outside the bias window for all molecules in the negative voltage range (left column in Fig. 8), but shifts more and more into this window at positive bias when going from M6 to M8 (arrows have been inserted in the right column of Fig. 8 as a guide to the eyes). This observation fully supports our previous conclusion that a structure-dependent energy shift of the LUMO is responsible for the trends of RR found in Figure 5. Our findings are of course limited to the range of molecules investigated in this article and should not be readily generalized to other unimolecular rectifiers. However, as pointed out before, our choice of systems exhibits many of the characteristic structural features found in previously studied unimolecular rectifiers,[16–18] namely a π-conjugated molecular backbone, nitro and amino groups, dithiolate anchoring groups and gold (111) surfaces as electrodes.
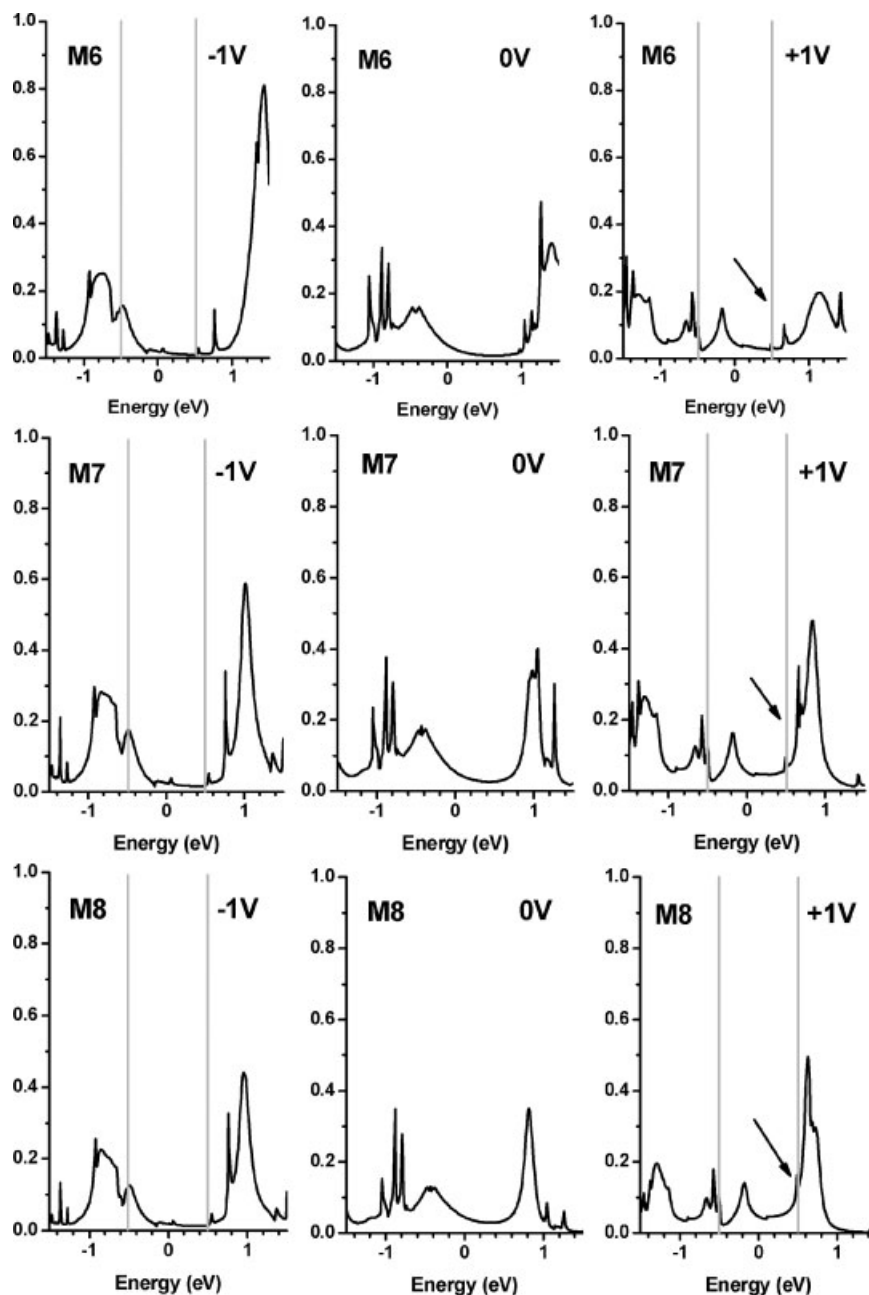
Figure 8. Transmission functions for molecules M6 (first row), M7 (second row), and M8 (third row) as calculated with the NEGF-DFT formalism. The plots are obtained for voltages of −1V (left column), 0V (middle column) and +1V (right column), respectively. The vertical bright lines indicate the bias window.

Figure 8 also highlights that electron transport occurs in the coherent regime for all metal/molecule/metal junctions investigated here due to the rather strong coupling of the thiol anchoring groups to both the π-electrons of the organic molecules and the s-electrons of the gold electrodes. This can be seen from the widths of all relevant peaks in Figure 8 that are larger than ∼0.5 eV. It would be interesting to determine whether RR would change for weaker couplings (a different choice of anchoring groups might reduce the coupling and the width of the transmission peaks, thereby shifting the electron

transport regime towards a Coulomb blockade behavior). This study is however, clearly beyond the scope of the present work.

4. Conclusions

In summary, we have presented a detailed investigation of structure-property relationships for unimolecular rectifiers and have explained the evolution of the rectification ratio among the structures from simple electrostatic arguments combined to a quantum-chemical insight derived from electronic structure

calculations. Our main conclusions relate to the outcome of the analysis of the structure-dependent rectification ratios and of a comparison of the ability of two conceptually very different computational techniques, AM1 and NEGF-DFT, to capture such characteristics.

4.1. Trends in the Rectification Ratios

In order to achieve a deep understanding of the effect of substituents on unimolecular rectification, it is not sufficient to just look at zero-bias properties such as donor and acceptor strengths. The relative position of the functional groups along the generated electrostatic potential also plays a very crucial role. This finding contrasts with design schemes for molecular rectifiers proposed in the past[16] and might also offer an explanation for the varying performance of recently investigated molecular diodes.[17,18] It is not necessarily only the HOMO and LUMO levels that participate in the rectification mechanism due to the fact that MOs further away from the Fermi energy can become important due to their highly localized nature and asymmetric position which both contribute in increasing the slope of their energetic evolution as a function of the bias. When an occupied or unoccupied level, which is energetically far from the HOMO-LUMO gap at zero bias, is involved, the trends derived from electrostatic arguments for the MOs next to the gap can be partially diminished or probably even reversed.

4.2. Comparison between AM1 and NEGF-DFT

Quantum-chemical calculations of intramolecular charge transfer processes at the AM1 level[33,34] seem to be a computationally efficient tool to investigate the trends for rectification, at least for the range of asymmetric molecules under consideration; the trends derived at the AM1 level were indeed found to be corroborated by more sophisticated (and computationally much more expensive) NEGF-DFT-based electron transport calculations,[9,35] which also include a proper treatment of the coupling of MOs to the electrodes. Although we cannot generalize this statement beyond the range of molecules that we have studied, this range exhibits nevertheless the characteristic structural features of many unimolecular rectifiers currently under investigation.[16–18] Our findings also suggest that the energetic alignment between MOs and the Fermi level of electrodes is not the only decisive factor when the rectification properties of different molecules are compared; our results clearly point to an intramolecular origin of the rectification mechanism, which is in deep contrast to the original Aviram-Ratner proposal.[1]

The physical origin for the close correspondence between the values for RR computed from the two approaches is not self evident, since there is no need for explicit level crossings in NEGF-DFT while there is with AM1. The common denominator between the two methods is actually the change in the slope of the field-evolution of the energy of specific MOs. If the slope is increased for an MO close to the Fermi energy in

the forward bias direction, it leads to a crossing occurring more easily with AM1 and to the corresponding level entering more easily into the bias window at low voltages for NEGF-DFT. In both methods, this contributes in establishing a RR if such an effect does not also occur in the reversed bias direction.

An interesting topic, which we will address in our future research, is to determine whether the close agreement of the results provided by the two techniques holds only for RR as small as those obtained for the range of molecules in our study or whether it applies for any unimolecular rectifier in general. For technological reasons, another goal is to design systems with substantially higher RR values than the ones discussed in this article.

[1] A. Aviram, M. A. Ratner, *Chem. Phys. Lett.* **1974**, *29*, 277.

[2] D. M. Eigler, E. K. Schweizer, *Nature* **1991**, *344*, 56.

[3] H. Ohnishi, Y. Kondo, K. Takayanagi, *Nature* **1998**, *344*, 524.

[4] C. Joachim, J. K. Gimzewski, A. Aviram, *Nature* **2000**, *408*, 541.

[5] C. Joachim, J. K. Gimzewski, R. R. Schlittler, C. Chavy, *Phys. Rev. Lett.* **1995**, *74*, 2102.

[6] M. A. Reed, C. Zhou, C. J. Muller, T. P. Burgin, J. M. Tour, *Science* **1997**, *278*, 252.

[7] J. Reichert, R. Ochs, D. Beckmann, H. B. Weber, M. Mayor, H.v. Löhneysen, *Phys. Rev. Lett.* **2002**, *88*, 176804.

[8] R. H. M. Smit, Y. Noat, C. Untiedt, N. D. Lang, M. C. van Hemert, J. M. van Ruitenbeek, *Nature* **2002**, *419*, 906.

[9] M. Brandbyge, J. L. Mozos, P. Ordejon, J. Taylor, K. Stokbro, *Phys. Rev. B* **2002**, *65*, 165401.

[10] Y. Xue, S. Datta, M. A. Ratner, *Chem. Phys.* **2002**, *281*, 151.

[11] Y. Fujimoto, K. Hirose, *Phys. Rev. B* **2003**, *67*, 195315.

[12] A. Calzolari, N. Marzari, I. Souza, M. B. Nardelli, *Phys. Rev. B* **2004**, *69*, 035108.

[13] A. R. Rocha, V. M. Garcia-Suarez, S. W. Baily, C. J. Lambert, J. Ferrer, S. Sanvito, *Nat. Mater.* **2005**, *4*, 335.

[14] L. V. Keldysh, *Sov. Phys. JETP* **1965**, *20*, 1018.

[15] Y. Meir, N. S. Wingreen, *Phys. Rev. Lett.* **1992**, *68*, 2512.

[16] J. C. Ellenbogen, J. C. Love, *Proc. IEEE* **2000**, *88*, 386.

[17] K. Stokbro, J. Taylor, M. Brandbyge, *J. Am. Chem. Soc.* **2003**, *125*, 3674.

[18] A. Staykov, D. Nozaki, K. Yoshizawa, *J. Phys. Chem. C* **2007**, *111*, 11699.

[19] R. M. Metzger, H. Tachibani, X. Wu, U. Hoepfner, B. Chen, M. V. Lakshmikantham, M. P. Cava, *Synth. Met.* **1997**, *85*, 1359.

[20] S. Lenfant, D. Guerin, F. Tran Van, C. Chevrot, S. Palacin, J. P. Bourgoin, O. Bouloussa, F. Rondelez, D. Vuillaume, *J. Phys. Chem. B* **2006**, *110*, 13947.

[21] G. J. Ashwell, A. Mohib, *J. Am. Chem. Soc.* **2005**, *127*, 16238.

[22] J. W. Ying, A. Cordova, T. Y. Ren, G. L. Xu, T. Ren, *Chem. Eur. J.* **2007**, *13*, 6874.

[23] R. M. Metzger, *Chem. Phys.* **2006**, *326*, 176.

[24] V. Mujica, M. A. Ratner, A. Nitzan, *Chem. Phys.* **2002**, *281*, 147.

[25] J. Taylor, M. Brandbyge, K. Stokbro, *Phys. Rev. Lett.* **2002**, *89*, 138301; A. Grigoriev, J. Sköldberg, G. Wendin, Z. Crljen, *Phys. Rev. B* **2006**, *74*, 045401.

[26] F. Zahid, A. W. Ghosh, M. Paulsson, E. Polizzi, S. Datta, *Phys. Rev. B* **2004**, *70*, 245317.

[27] P. E. Kornilovitch, A. M. Bratkovksy, R. S. Williams, *Phys. Rev. B* **2002**, *66*, 165436.

[28] M. Galperin, A. Nitzan, S. Sek, M. Majda, *J. Electroanal. Chem.* **2003**, *550*, 337.

[29] B. Song, D. A. Ryndyk, G. Cuniberti, *Phys. Rev. B* **2007**, *76*, 045408.

[30] A. A. Kornyshev, A. M. Kuznetsov, J. Ulstrup, *Proc. Nat. Acad. Sci.* **2006**, *103*, 6799.

[31] E. G. Petrov, Y. R. Zelinsky, V. May, P. Hänggi, *J. Chem. Phys.* **2007**, *127*, 084709.

[32] A. Broo, M. C. Zerner, *Chem. Phys.* **1995**, *196*, 423.

[33] AMPAC 8, Semichem, Inc, Shawnee KS **2004** (www.semichem.com); a full CI has been performed in an active space built from the highest five and lowest five MOs for all molecules investigated with AM1 in this study.

[34] M. J. S. Dewar, E. G. Zoebisch, E. F. Healy, J. J. P. Stewart, *J. Am. Chem. Soc.* **1985**, *107*, 3902.

[35] Atomistix ToolKit version 2.2, Atomistix A/S, Copenhagen, Denmark **2004** (www.atomistix.com).

[36] J. M. Soler, E. Artacho, J. D. Gale, A. Garcia, J. Junquera, P. Ordejon, D. Sanchez-Portal, *J. Phys.: Condens. Matt.* **2002**, *14*, 2745.

[37] J. Gottschalck, B. Hammer, *J. Chem. Phys.* **2002**, *116*, 784.

[38] A. Bilic, J. R. Reimers, N. S. Hush, *J. Chem. Phys.* **2005**, *122*, 094708.

[39] M. J. Frisch, G. W. Trucks, H. B. Schlegel, P. M. W. Gill, B. G. Johnson, M. A. Robb, J. R. Cheeseman, T. Keith, G. A. Petersson, J. A. Montgomery, K. Raghavachari, M. A. AlLaham, V. G. Zakrzewski, J. V. Ortiz, J. B. Foresman, J. Cioslowski, B. B. Stefanov, A. Nanayakkara, M. Challacombe, C. Y. Peng, P. Y. Ayala, W. Chen, M. W. Wong, J. L. Andres, E. S. Replogle, R. Gomperts, R. L. Martin, D. J. Fox, J. S. Binkley, D. J. Defrees, J. Baker, J. P. Stewart, M. Head-Gordon, C. Gonzalez, J. A. Pople, Gaussian 98, Revision A.11.3, Gaussian, Inc, Pittsburgh PA **2002** (www.gaussian.com).

[40] J. P. Perdew, R. G. Parr, M. Levy, J. L. Balduz, *Phys. Rev. Lett.* **1982**, *49*, 1691; W. Kohn, *Phys. Rev. B* **1986**, *33*, 4331.

[41] S. Datta, W. Tian, S. Hong, R. Reifenberger, J. I. Henderson, C. P. Kubiak, *Phys. Rev. Lett.* **1997**, *79*, 2530.

[42] C. Krzeminski, C. Delerue, G. Allan, D. Vuillaume, R. M. Metzger, *Phys. Rev. B* **2001**, *64*, 085405.

[43] M. Elbing, R. Ochs, M. Koentopp, M. Fischer, C.v. Hänisch, F. Weigend, F. Evers, H. B. Weber, M. Mayor, *Proc. Nat. Ac. Sci.* **2005**, *102*, 8815.